Journal of Pharmaceutical Analysis 14 (2024) 100995

Contents lists available at ScienceDirect

Journal of Pharmaceutical Analysis

journal homepage: www.elsevier.com/locate/jpa

Original article

Optical biosensing of monkeypox virus using novel recombinant silica-binding proteins for site-directed antibody immobilization

Xixi Song [1], Ying Tao [1], Sumin Bian **, Mohamad Sawan *

CenBRAIN Neurotech, School of Engineering, Westlake University, Hangzhou, 310030, China

ARTICLE INFO

Article history:
Received 30 January 2024
Received in revised form
26 April 2024
Accepted 29 April 2024
Available online 7 May 2024

Keywords:
Site-directed immobilization
Silica-binding proteins
Optical biosensing
Monkeypox virus
Spiked clinical samples
Multi-virus biosensor

ABSTRACT

The efficient immobilization of capture antibodies is crucial for timely pathogen detection during global pandemic outbreaks. Therefore, we proposed a silica-binding protein featuring core functional domains (cSP). It comprises a peptide with a silica-binding tag designed to adhere to silica surfaces and tandem protein G fragments (2C2) for effective antibody capture. This innovation facilitates precise site-directed immobilization of antibodies onto silica surfaces. We applied cSP to silica-coated optical fibers, creating a fiber-optic biolayer interferometer (FO-BLI) biosensor capable of monitoring the monkeypox virus (MPXV) protein A29L in spiked clinical samples to rapidly detect the MPXV. The cSP-based FO-BLI biosensor for MPXV demonstrated a limit of detection (LOD) of 0.62 ng/mL in buffer, comparable to the 0.52 ng/mL LOD achieved using a conventional streptavidin (SA)-based FO-BLI biosensor. Furthermore, it achieved LODs of 0.77 ng/mL in spiked serum and 0.80 ng/mL in spiked saliva, exhibiting no cross-reactivity with other viral antigens. The MPXV detection process was completed within 14 min. We further proposed a cSP-based multi-virus biosensor strategy capable of detecting various pandemic strains, such as MPXV, the latest coronavirus disease (COVID) variants, and influenza A protein, to extend its versatility. The proposed cSP-modified FO-BLI biosensor has a high potential for rapidly and accurately detecting MPXV antigens, making valuable contributions to epidemiological studies.

1. Introduction

Global responses to pandemics emphasize the critical need for biosensors to monitor outbreaks during major public health events [1]. The monkeypox virus (MPXV) pandemic is spreading, and the number of MPXV infections and deaths worldwide continues to grow. As of December 19, 2023, 116 countries and regions have confirmed 92,783 cases and 171 deaths, according to the World Health Organization (WHO) [2]. MPXV infections emphasize the need for rapid and sensitive pathogen diagnostics. This action is crucial for guiding timely and effective clinical treatments and vaccination strategies in the face of this evolving public health challenge [3,4]. However, current detection technologies, including real-time polymerase chain reaction (PCR) (real-time PCR) tests and isothermal amplification-related methods [5], are flawed because they require rigidly structured environments and well-trained personnel to perform the precise steps. Therefore, an easy, rapid, and automated biosensing method to efficiently detect MPXV in clinical samples is required.

Immunosensors, a subset of biosensors relying on antibody-target affinity, have demonstrated diverse applications in medical diagnostic testing, from classical disease biomarkers to pathogenic viruses [6–8]. Among the existing immunosensing technologies, silica nanomaterials have been extensively used to construct robust and low-cost optical/electrochemical biosensors for monitoring various viruses because of their lower energy loss compared with metallic media [9,10]. Strategies for immobilizing antibodies on natural silica surfaces typically include physical adsorption, bio-affinity immobilization, and covalent binding [11]. Among these methods, affinity-based antibody immobilization using protein A/G stands out because it can enable site-directed immobilization while preserving the biological activity of the antibody and enhancing antigen capture, which is essential for maintaining biosensing consistency and processing reproducibility [12]. In addition, utilizing only key structural domains (Z domain of protein A [13], or C2 domain of protein G [14]) rather than whole-sized proteins is economical and enhances antibody density on silica surfaces.

Notably, careful attention to the conditions of protein A/G immobilization is crucial, as they significantly influence subsequent

Peer review under responsibility of Xi'an Jiaotong University.

* Corresponding author.
** Corresponding author.
E-mail addresses: biansumin@westlake.edu.cn (S. Bian), sawan@westlake.edu.cn (M. Sawan).

[1] Both authors contributed equally to this work.

https://doi.org/10.1016/j.jpha.2024.100995

antibody loading and biosensing performance. This requires special bridging compounds such as thiol groups, biotin labels, and peptides to reduce the effect of the interface on the protein A/G [15]. Silica-binding peptides (Si-tags) have been identified as potent tools for coating silica surfaces with proteins A/G, which exhibit a subnanomolar dissociation constant. Kim et al. [16] emphasized the efficacy of a shorter tag containing the essential functional part of the Si-tag and demonstrated its superior performance in assisting the immobilization of partner proteins on silica.

Unfortunately, functional and application studies on recombinant proteins consisting of the core structural domains of proteins A/G and Si-tags are lacking. This gap in the knowledge negatively affected the opportunity to discover efficient and cost-effective tools for antibody immobilization. We introduced a silica-binding protein featuring core functional domains (cSP) to address these challenges. The innovative protein comprises a Si-tag designed to adhere to silica surfaces, along with tandem protein G fragments (2C2) for efficient antibody capture. This construct facilitates site-directed immobilization of specific monoclonal antibodies (mAbs) onto silica surfaces through robust irreversible adsorption following a simple incubation process. Next, in the efforts to detect MPXV in clinical settings, we applied cSP to silica-coated optical fibers and established a fiber-optic biolayer interferometer (FO-BLI) biosensor capable of monitoring MPXV protein A29L in spiked clinical samples. FO-BLI biosensors have recently demonstrated their utility in rapidly detecting neutralizing antibodies in vaccinated donors [17,18], severe acute respiratory syndrome coronavirus 2 (SARS-CoV-2) antigens [19], and small-molecule drugs [20] in clinical samples using streptavidin (SA)-based optical fibers for mAb capture and target detection.

Despite the proven efficiency of the SA-biotin-based mAb functionalization strategy for rapid and sensitive target detection, it exhibits two main limitations. First, it may lead to less oriented binding of mAbs owing to their conjugation with biotins. Second, its adaptation to other silica surface-based optical fiber platforms is time-consuming. Consequently, in this paper, we present three main novelties: 1) versatile recombinant silica-binding proteins for the site-directed immobilization of mAbs directly on silica surfaces; 2) leveraging the FO-BLI biosensor as a platform to demonstrate the utility of cSP for the rapid and sensitive detection of MPVX in clinical settings; and 3) a cSP-based multi-virus biosensing strategy for detecting diverse pandemic strains, such as MPXV, coronavirus disease (COVID) variants, and influenza A protein, within a single sample.

2. Materials and methods

2.1. Materials, buffers, and equipments

Information on the antibodies and antigens used in this study is summarized in Table S1. The Biotin Conjugation Kit (ab201796) and Horseradish Peroxidase (HRP) Conjugation Kit (ab102890) were purchased from Abcam (Cambridge, UK). The 3-amino-9-ethylcarbazole (AMEC) Red Substrate Kit (SK-4285) was purchased from VectorLabs (Shanghai, China). The BL21 (DE3) (C504-03) was purchased from Vazyme (Nanjing, China). The Luria-Bertani (LB) liquid medium (B540111) and LB Agar Plate (B530113) were purchased from Sangon Biotech (Shanghai, China). The kanamycin (ST102), isopropyl β-D-1-thiogalactopyranoside (IPTG, ST098-1g), His-tag Protein Purification Kit (P2226), BeyoGel 15% polyacrylamide gel electrophoresis (PAGE) Gel (P0461S), Coomassie blue fast staining solution (P0017), prestained color protein ladder (P0078), 10× sodium dodecyl sulfate (SDS)-PAGE buffer with Tris-Gly (P0014D), and SDS-PAGE loading buffer (P0286) were purchased from Beyotime Biotech Inc. (Shanghai, China). The 30% H_2O_2 (10011208) and 25%–28% ammonia (10002118) were purchased from Sinopharm Group (Shanghai, China). Bovine serum albumin (BSA; SRE0096-50G) and Tween-20 (11332465001) were purchased from Sigma-Aldrich (Shanghai, China).

The oxidizing liquid (deionized (DI) water:30% H_2O_2:25%–28% ammonia (3:1:1, *V*/*V*/*V*)), phosphate-buffered saline (PBS, 10 mM, pH 7.4), sample diluent (SD) buffer (PBS buffer containing 0.1% (*V*/*V*) BSA and 0.02% (*V*/*V*) Tween-20), and high-salt SD buffer (SD buffer containing 274 mM NaCl) were freshly prepared in house. All solutions were prepared using DI water purified by Milli-Q (Merck KGaA, Darmstadt, Germany). The Octet K2 2-channel system (Octet system) and SA-coated fibers were purchased from Sartorius (Gottingen, Germany).

2.2. Expression and purification of cSP

The coding sequence of recombinant cSP was synthesized and cloned into pET26b (+) at the *NdeI*/*XhoI* site to form the pET26b-*cSP* plasmid (GenScript, Nanjing, China), which was then transformed into BL21(DE3) cells. A single colony was cultured in 4 mL of LB liquid medium with 10 μg/mL kanamycin at 37 °C, 200 rpm (~0.6 optical density (OD_{600})), and 1 mL of the culture was transformed into 100 mL of fresh kanamycin-contained LB liquid medium for subculturing and induced with 0.05 mM IPTG (~0.6 OD_{600}) for 16 h at 15 °C, 180 rpm. Then, cells were harvested by centrifugation at 4,000 rpm and 4 °C for 20 min and washed twice with PBS buffer. The cSP protein was purified according to the instructions of the His-tag Protein Purification Kit and analyzed using 15% SDS-PAGE gel.

2.3. Prediction of the cSP structure

The three-dimensional (3D) structure of the cSP protein was predetermined using Modeller 10.4 software in the Python environment [21] with SWISS-MODEL [22,23] for template identification. All steps followed the tutorial on the Modeller website (https://salilab.org/modeller/). The final structure was visualized using PyMOL.

2.4. Preparation of the bare silica-coated optical fibers

Commercially available SA-coated fibers were transformed into bare silica-coated optical fibers following the procedure outlined by Liu et al. [24]. Briefly, the SA-coated fibers were immersed in the oxidizing liquid (DI water:H_2O_2:ammonia (3:1:1, *V*/*V*/*V*)) at 80 °C, and all the converted bare-silica fibers were stored in 20% (*V*/*V*) ethanol and underwent rinsing in DI water before utilization. The optimal treatment time was determined using an Octet system. The silica-coated fibers were treated under a series of treatment times: 30, 60, 90, and 120 min. The fibers were rinsed twice with DI water. After this, all treated fibers were submerged in the cSP solution for 80 s, following a 60-s washing step with SD buffer. The fibers were then dipped into the wells with the mAb solution for 80 s for mAb loading. After another 60-s washing step, all cSP-mAb-coated fibers were immersed in the antigen solution for 80 s. The amount of binding at each step was assessed using the relative wavelength shift. The cSP solution (5 μg/mL), mAb solution (10 μg/mL), and antigen solution (1 μg/mL) were prepared using SD buffer for use in this step. All steps were performed at 25 °C, with a shaking speed of 400 rpm.

2.5. Affinity of cSP-modified optical fibers to different antibodies

Both the cSP and mAb solutions (5 and 10 μg/mL, respectively) were prepared using SD buffer. All the mAbs from humans, goats, donkeys, rabbits, and mice are summarized in Table S1. The measurement process was similar to that presented in Section 2.4, using the Octet system, whereas the cSP affinity to mAbs was assessed by the relative wavelength shift.

2.6. Establishing a cSP-based biosensor for MPXV protein A29L detection in buffer and spiked clinical samples

At first, silica-coated fibers were immersed into SD buffer and washed by shaking for 60 s and afterward submerged in 5 μg/mL cSP solution for 80 s loading step following the washing step. For specifically recognizing and binding the antigen, fibers were loaded with 10 μg/mL capture antibody (1st mAb), which was dipped into the wells with 1st mAb solution for 80 s. After another 60-s washing step, all cSP-mAb-coated fibers were immersed in the antigen solution for 80 s. The antigens were diluted to 0, 1, 5, 10, 20, 50, and 100 ng/mL. Next, antigen-modified fibers were submerged into the 1.25 μg/mL HRP-conjugated detection antibody (2nd mAb) after another washing step. The signal was finally enhanced using an AMEC signal enhancer, a compound that can react with HRP to produce a precipitate for signal enhancement [19].

The antigens were also detected in two other matrices: blank serum and saliva. When applying cSP-based fibers to a complex matrix, the matrix effect on the biosensing performance needs to be considered. Serum and saliva were diluted with high-salt SD buffer, as evaluated in another study by our team, to reduce matrix effects and non-specific binding [20]. For saliva, the dilution factor was evaluated using 10-, 20-, and 30-fold tests. A 20-fold dilution was selected as most appropriate. A previous study [17] reported that the serum was diluted 100-fold. Finally, the antigens were dissolved in the two matrices and diluted with high-salt SD buffer to obtain gradient concentrations of 100× diluted serum and 20× diluted saliva containing antigen at 0, 1, 5, 10, 20, 50, and 100 ng/mL. The amount of binding at each step was assessed using the relative wavelength shift.

2.7. Specificity of the MPXV FO-BLI biosensors

Specificity was evaluated using three different pandemic viruses, i.e., SARS-CoV-2, vaccinia virus (VACV), and influenza A, at 5 ng/mL (details shown in Table S1). Before detection, each cSP-based fiber was uniformly conjugated with the mAbs targeting MPXV. Subsequently, these fibers were immersed in the three viral solutions and blank control buffer. Signal amplification was performed using HRP-conjugated 2nd mAbs. Cross-reactivity between the 1st mAbs and 2nd mAbs against any of the viruses will be reflected in the results as a significant shift.

2.8. Comparison of cSP-based sensor and commercial SA sensor

The SA-coated fiber, a widely used fiber covered with SA, was compared with the cSP-based sensor. It was biotinylated according to the biotinylation manual to immobilize the 1st mAbs against MPXV on the SA fibers. The mAbs were mixed with biotinylation reagents and shaken in the dark at room temperature (20–25 °C) for 30 min. The 2nd mAbs were combined with HRP conjugation reagent, gently shaken, and incubated in the dark for more than 3 h at room temperature. In contrast to the SA-coated fibers, the cSP-based fibers are composed of silica, requiring an additional step of loading the cSPs onto the bare silica fibers for subsequent binding to the 1st mAbs. The 1st mAbs were immobilized onto SA-coated and cSP-based fibers. Following a washing step, all the mAb-coated fibers were submerged in MPXV A29L protein at various concentrations: 0, 1, 5, 10, 20, 50, and 100 ng/mL. The 2nd mAbs labeled with HRP were used to amplify the signal.

2.9. Data analysis

The limit of detection (LOD) is defined as the antigen concentration equal to the average of the blank plus three times the standard deviation. This value was calculated using the following equation:

$$y = x \times A/(x + B)$$

where x is the concentration of the target, y is the binding shift, and A and B represent the fitting parameters. We input the "blank shift + 3 × standard deviation (STD)" as "y" into the formula to obtain LOD; the blank shift is the data of the blank group, and the STD is the standard deviation of non-specific binding ($n > 3$). Statistical analyses were performed using GraphPad Prism 9.02 (GraphPad Software, San Diego, CA, USA), following the "nonlinear regression and one-site specific binding" mode.

3. Results

3.1. Design and preparation of the recombinant cSP

The newly designed recombinant cSP contains two core functional domains validated in previous studies: the recombinant protein G (2C2), renowned for its affinity for antibody binding (comprising two units [25] of the C2 fragment of protein G, Protein Data Bank (PDB) ID: 1FCC), and the innovatively redesigned ribosomal protein L2 (Si-tag), which actively contributes to silica binding [16]. A flexible linker was introduced at the C-terminus of 2C2 for fusion with the Si-tag (Fig. 1A). Subsequently, the coding sequence of the cSP protein was inserted into pET26b (+) at the *NdeI*/*XhoI* site, enabling its expression through *Escherichia coli* (*E. coli*) and facilitating purification via the C-terminal His_6-tag (as illustrated in Fig. 1B). The purified cSP protein was analyzed using SDS-PAGE, which revealed a molecular weight of 29.47 kDa (Fig. 1C).

3.2. Verification of cSP immobilizes antibodies onto bare silica

We validated the functionality of the cSP and investigated its loading conditions using an optical system. First, we prepared FO-BLI bare silica fibers and confirmed that cSP effectively adhered to the silica surfaces and efficiently captured the mAbs. Notably, the duration of the oxidizing treatment emerged as a crucial parameter influencing bare-silica fiber conversion. As shown in Fig. 2A, an extended treatment time resulted in higher wavelength shifts during cSP loading and mAb capture. Intriguingly, the wavelength shifts for mAb capture and antigen association were similar after 90 and 120 min of oxidative treatment. Thus, we used 90 min-treated bare silica fibers for cSP modification. Optimal binding saturation was achieved by fine-tuning the cSP/mAb concentration and binding time (Fig. 2B).

A special SD buffer was used to minimize non-specific adsorption [19]. Binding conditions involved cSP (5 μg/mL) for 80 s and mAb (10 μg/mL) for 60 s, and each binding step was supplemented with a 60-s wash. Subsequently, we evaluated the binding capabilities of the cSP-modified bare silica fibers with mAbs from various species. Two mAbs each from humans, goats, donkeys, rabbits, and mice were used for this assessment. The results revealed that the cSP-modified bare-silica fibers exhibited robust binding across diverse species of mAbs, demonstrating a binding trend similar to that reported for protein G [26] (Fig. 2C).

3.3. Establishing the cSP-based FO-BLI biosensor for MPXV detection

The cSP-based immobilization of antibodies represents a streamlined, eco-friendly, and efficient minimal biofunctionalization approach that simplifies the process by requiring bare silica fibers to

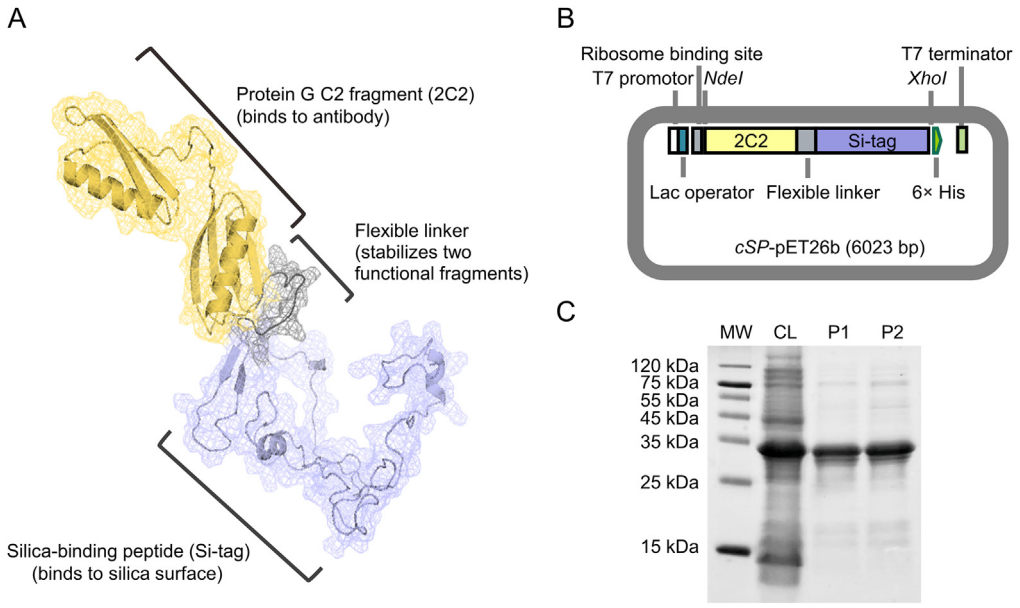

Fig. 1. Scheme for designing and purifying recombinant silica-binding protein featuring core-functional domains (cSP). (A) Schematic of the three-dimensional (3D) structure of cSP projected through Modeller10.4. (B) The structural diagram of the implemented *cSP* fusion gene in the pET26b plasmid. The *cSP* expression was regulated by the T7 promoter with a lac operator. (C) Validation of cSP expression and purification via sodium dodecyl sulfate-polyacrylamide gel electrophoresis (SDS-PAGE). 2C2: tandem protein G fragments; Si-tag: silica-binding peptide. MW: molecular weight marker; CL: whole-cell lysate; P1 and P2: purified cSP proteins.

undergo sequential immersion in cSP and antibody solutions, eliminating the need for additional chemical treatments. A comparative analysis of its advantages over traditional methods is presented in Table 1. We established a cSP-based FO-BLI biosensor tailored for MPXV detection to emphasize the versatility of cSP in biosensing applications. This assay specifically targeted the A29L antigen of MPXV across diverse media, including buffer, serum, and saliva, as described in the flowchart in Table 2 and Fig. 3.

The sample-to-result time for cSP-based biosensing in the SD buffer was optimized to within 12 min. In this case, the capture antibody (1st mAb) was coated onto the bare silica fiber via cSP, accomplished within 340 s. Then, the MPXV A29L protein was diluted in SD buffer, presenting a concentration gradient ranging from 0 to 100 ng/mL with a rapid 140-s detection phase. The concentration of the HRP-conjugated detection antibody (2nd mAb-HRP) and the dilution factor of the AMEC enhancer were adjusted to control for background interference (~1 nm) and maximum positive signal (~40 nm for 100 ng/mL of A29L) during a 220-s signal amplification period.

3.4. The cSP-based FO-BLI biosensor for MPXV detection in buffer and spiked clinical samples

We plotted standard curves using two pairs of mAbs (designated as MPXV-Ab pairs) targeting the MPXV A29L protein, as shown in Fig. 4A. MPXV-Ab pair 1 (M29-27 and M29-26-HRP) exhibited superior signal values and lower LOD. The specificity of the mAb pair was assessed using three pandemic virus proteins: VACV A27L homologous to MPXV A29L, SARS-CoV-2 XBB.1.5 receptor-binding domain (RBD), and influenza A H3N2 (H3N2) nucleoprotein, at a concentration of 5 ng/mL. As shown in Fig. 4B, the cSP-based biosensor did not cross-react with any viral proteins other than MPXV.

We further loaded the optimal mAb pair (M29-27 and M29-26-HRP) onto the commercial SA-coated FO-BLI biosensor and compared its detection performance with that of the cSP-based biosensor. As shown in Fig. 4C, the signal trends and LOD of cSP-based biosensing (0.62 ng/mL) are close to those of SA-based biosensing (0.52 ng/mL). This convergence in performance confirmed the high reliability of cSP-based biosensing.

We used a high-salt SD buffer for sample dilution to mitigate potential non-specific interference from serum and saliva components on the sensor. Standard curves for MPXV A29L protein in 100-fold serum and 20-fold saliva samples were generated using the above-defined detection parameters (Fig. 4D, $R^2 = 0.9959$ in serum; $R^2 = 0.9906$ in saliva). A29L concentrations ranging from 0 to 100 ng/mL were detected in diluted serum and saliva, and the LODs were 0.77 ng/mL in serum and 0.80 ng/mL in saliva.

A comparative analysis of the assay performance of the cSP-based FO-BLI biosensor with other excellent optical biosensors was summarized in Table 3 [27–30]. To the best of our knowledge, this is the first time that a cost-effective cSP protein has been used for silica surface modification and represents a new direction for MPXV detection. Comparative aspects include the types and immobilization methods of the recognition elements, sensing approaches, turnaround time, detection matrices, and detection throughput. The cSP-based FO-BLI platform exhibits notable advantages, including rapid detection speed (from antibody loading to output results, <15 min), high sensitivity in real samples (achieving a low LOD comparable to the buffer in both serum and saliva), and high-throughput capacity (diverse sample and multi-antigen detection using the eight-channel system).

3.5. Perspective of the cSP-based multi-virus detection using optical platforms with silica surface

We proposed a high-throughput multiplexed detection technology utilizing a multi-channel FO-BLI system to demonstrate the adaptability of the recombinant cSP protein for multi-virus detection. Leveraging the impressive loading capacity of cSP proteins for mAbs, it has become seamless and robust for loading mAbs targeting various viruses. Capitalizing on the automated and streamlined sample-to-signal process facilitated by this system, a single run could accommodate eight viral assays for four samples within 15 min (Fig. 5A).

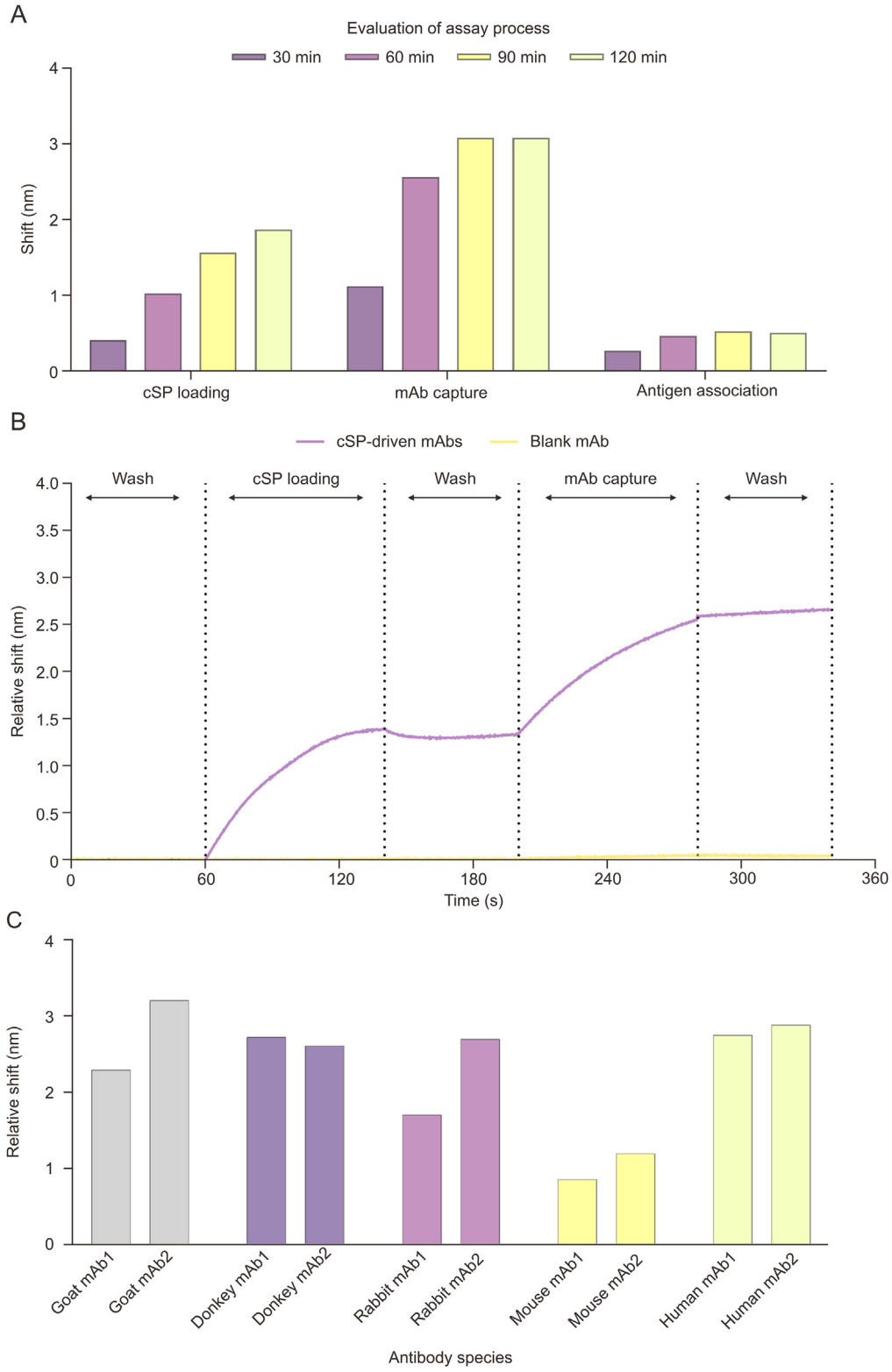

Fig. 2. Construction and characterization of the bare-silica fibers in silica-binding protein featuring core-functional domains (cSP)-based monoclonal antibody (mAb) loading on silica surface. (A) Evaluation of the optimized oxidizing treatment time on bare-silica fiber conversion. (B) Representative result of the cSP-driven mAbs loading on the fiber-optic biolayer interferometer (FO-BLI) biosensor using silica-coated fibers. (C) Validation of the cSP capacity in capturing mAbs generated from different species.

Furthermore, advances in multiplexed biosensors for addressing intricate epidemiological infections are limited by the limitations in bioreceptor modification. However, bioreceptors targeting different viruses are key subcomponents for achieving high selectivity in multiplexed biosensors [31]. The cSP-based site-directed antibody immobilization proposed in this study provides an important addition to the high-throughput immobilization of bioreceptors, thereby facilitating the bio-functionalization of multiplexed biosensing platforms with silica surfaces (Fig. 5B).

Table 1
Comparison of silica-binding protein featuring core-functional domains (cSP)-based immobilization and traditional covalent binding methods.

Categories	Covalent binding[a]	cSP-based immobilization
Surface pre-treatment	Yes	N/A
Chemical surface modification	Yes	N/A
Chemical linking	Yes	N/A
Site-direction	Depend on method	Yes
Time required	1 h to 1 day	~5 min
Price	Relatively high	Cost-effective
Safety	Require attention	Safe

[a] Examples of covalent binding include $-NH_2$/$-COOH$, $-SH$, etc. N/A: not applicable.

4. Discussion

This study introduced a novel and versatile recombinant silica-binding protein for the precise site-directed immobilization of mAbs directly on silica surfaces. The FO-BLI biosensor was used as a platform to demonstrate the utility of rapid and sensitive detection of MPVX in clinical settings. The recombinant cSP protein acts as an intermediary to enable interactions between the capture antibody and silica surfaces. Capture antibodies were immobilized onto silica surfaces via extremely robust charge adsorption with conformational adaptation [32], obviating the need for intricate chemical modification procedures. The specificity and sensitivity of the method were assessed by antibody detection and signal amplification using AMEC-HRP. In our investigations, MPXV A29L was assessed across a concentration range of 1–100 ng/mL in both serum and saliva, demonstrating no interference from other viral proteins. Remarkably low LODs of 0.77 ng/mL in serum and 0.80 ng/mL in saliva were achieved for MPXV detection in clinical settings.

Notably, the adaptability of this approach is highlighted by the ease with which cSP-based biosensing can be fine-tuned by substituting virus-specific antibodies. This feature allows for multi-virus detection without the need for extensive and complex steps to modify the capture antibodies. The FO-BLI system used in this study boasts automation and multichannel capabilities, streamlining the

Table 2
Protocols of the silica-binding protein featuring core-functional domains (cSP)-based fiber-optic biolayer interferometer (FO-BLI) biosensor to detect monkeypox virus (MPXV) in buffer, serum, and saliva.

Assay conditions		Buffer	Serum	Saliva
Immobilization of cSP and capture antibody	Probes	Silica-coated fibers	Silica-coated fibers	Silica-coated fibers
	cSP concentration (μg/mL)	5	5	5
	Load cSP shift (nm) ($n = 21$)	1.66 ± 0.09	1.71 ± 0.13	1.48 ± 0.09
	Loading time[a] (s)	80	80	80
	1st mAb concentration (μg/mL)	10	10	10
	Capture 1st mAb shift (nm) ($n = 21$)	0.96 ± 0.14	0.82 ± 0.08	0.77 ± 0.07
	Capture time (s)	80	80	80
Target detection	Sample dilution	N/A	1/100	1/20
	Matrix baseline (s)	60	200	200
	Incubation time[a] (s)	80	80	80
Signal amplification	2nd mAb concentration (μg/mL)	1.25	1.25	1.25
	Capture time[a] (s)	80	80	80
	Signal enhancer	1/10	1/10	1/10
	Enhancing time (s)	80	80	80
Assay properties	Detection range (ng/mL)	1–100	1–100	1–100
	Sample-to-result time (min)	12	14	14

[a] Each of these steps includes a 60-s wash. N/A: not applicable. mAb: monoclonal antibodies.

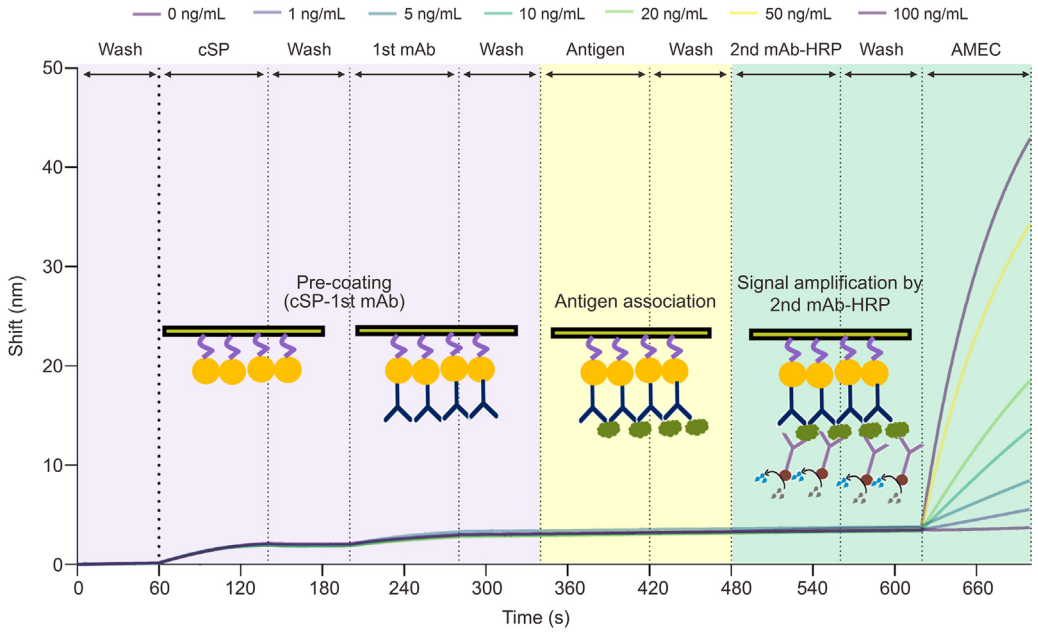

Fig. 3. Flowchart of the silica-binding protein featuring core-functional domains (cSP)-based monkeypox virus (MPXV) detection in buffer and spiked clinical samples. mAb: monoclonal antibody; HRP: horseradish peroxidase; AMEC: 3-amino-9-ethylcarbazole.

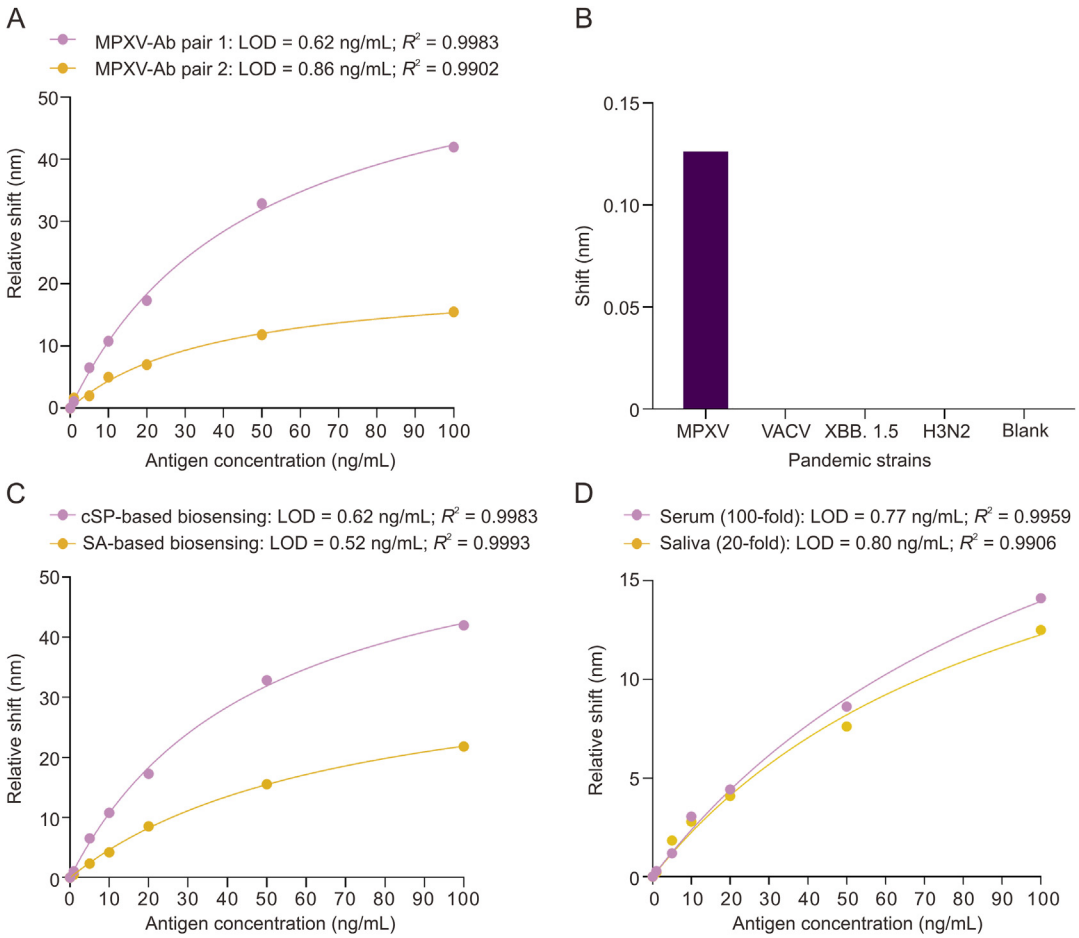

Fig. 4. The silica-binding protein featuring core-functional domains (cSP)-based fiber-optic biolayer interferometer (FO-BLI) biosensor for monkeypox virus (MPXV) detection in buffer and spiked clinical samples. (A) The MPXV antibody screening of cSP-based assay. (B) The cross-reactivity assay towards MPXV, vaccinia virus (VACV), severe acute respiratory syndrome coronavirus 2 (SARS-CoV-2) XBB.1.5 (XBB.1.5), and influenza A H3N2 (H3N2). (C) A comparison of the standard curves generated using the cSP-based vs. streptavidin (SA)-based biosensing strategy for MPXV detection in buffer. (D) The cSP-based biosensing performance for MPXV detection in spiked saliva and serum. MPXV-Ab: MPXV antibody; LOD: limit of detection.

entire process encompassing antibody loading, sample testing, and signal reading. This establishes a compelling case for achieving high-throughput, automated, and rapid multi-virus detection. Additionally, recombinant cSP has a versatile range of applications, particularly in facilitating multiple antibody modifications for multiplexed biosensing using silica interfaces. This represents a groundbreaking technology that has expedited hardware development.

Although cSP-based biosensors exhibit promising potential for rapid MPXV detection owing to their short runtimes and high-throughput capabilities, they still face several challenges and limitations. First, the effectiveness of this technique depends on the availability of virus-specific antibodies. This is due to an inherent drawback of the protein G structural domain of recombinant cSP, which lacks high affinity for all antibodies. Second, the demonstration in this study stopped with the testing of the spiked samples. Technological advancements will be pursued across three key directions to advance this strategy: 1) selecting specific antibody pairs tailored for various emerging viruses, including antibody-antibody and antibody-aptamer matches, or producing the

Table 3
Comparison of the assay performance for monkeypox virus (MPXV) detection between this work and other optical biosensors reported in the literature.

Target	Coupling agent	LOD (ng/mL)	Time (min)	Approaches	Refs.
A29L, A35R, M1R, and B6R	N/A	Buffer: 5 Serum: N/A	2	Surface-enhanced Raman spectroscopy	[27]
A29	N/A (physical adsorption, non-oriented)	Buffer: 0.05	10–15	Colorimetric/lateral flow	[28]
A35R	N/A (physical adsorption, non-oriented)	Buffer: 7.5 Serum: N/A	15	Fluorescent/lateral flow	[29]
A29	N/A (physical adsorption, non-oriented)	Buffer: 0.0024 Serum: N/A	15	Colorimetric-fluorescent dual-signal/lateral flow	[30]
A29L	cSP (affinity binding, oriented)	Buffer: 0.62 Serum: 0.77 Saliva: 0.80	12–14	Biolayer interferometry (high-throughput, multi-virus detection)	This work

N/A: not applicable. LOD: limit of detection; cSP: silica-binding protein featuring core-functional domains.

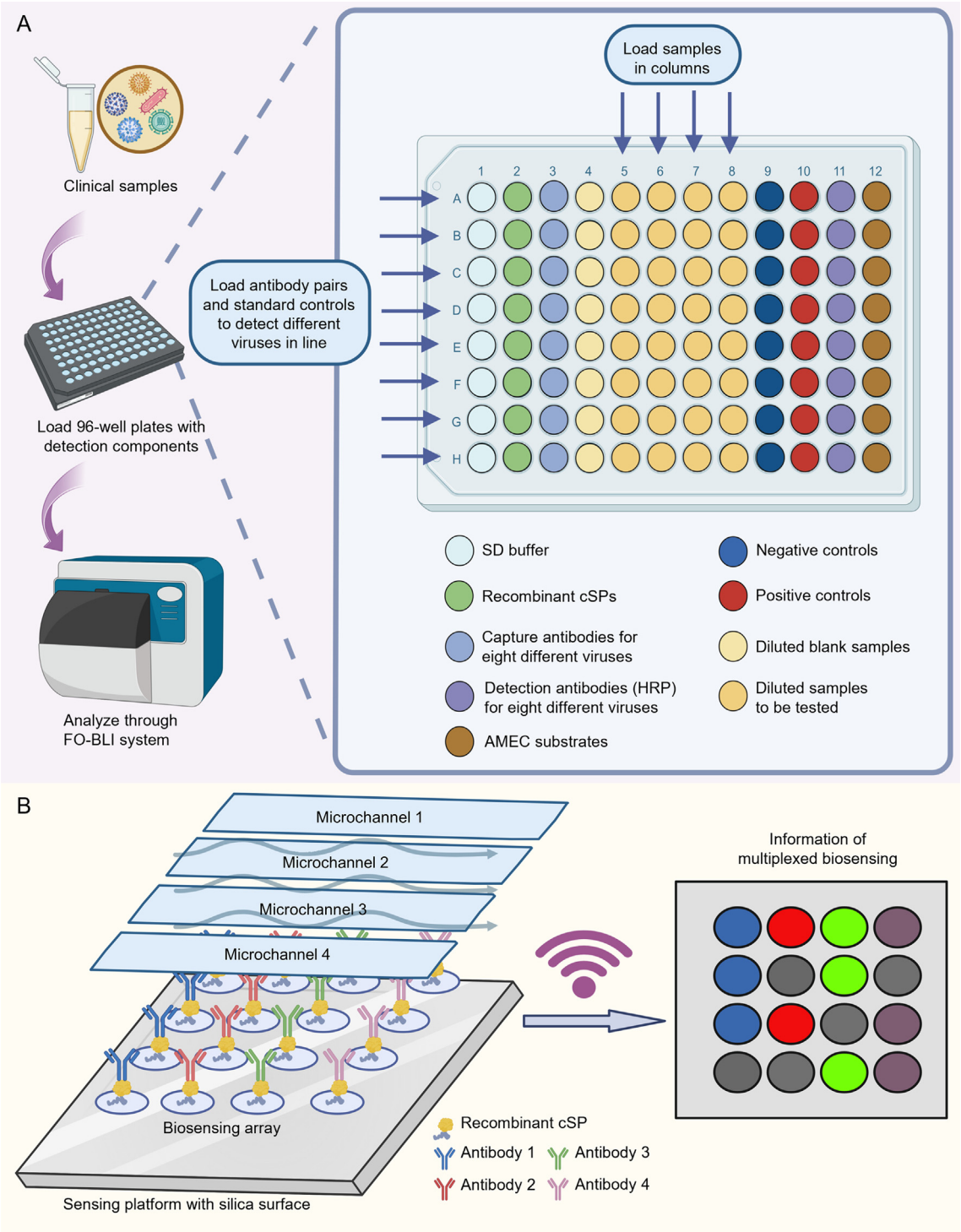

Fig. 5. Future perspective for multi-virus detection using the silica-binding protein featuring core-functional domains (cSP)-based optical biosensor. The cSP-based biosensing supports the loading of antibodies through a uniform and straightforward process. This capability enables the simultaneous detection of multiple viruses in one single sample, streamlining the analytical procedure. (A) The illustration depicts the sequential steps of loading antibodies, samples, and standards on a fiber-optic biolayer interferometer (FO-BLI) system. The entire assay supports the simultaneous detection of eight pathogens in four samples in less than 15 min. (B) The illustration shows high-throughput immobilization of antibodies using recombinant cSP on a biosensing platform with silica surface for multiplexed virus detection. SD buffer: sample diluent buffer; HRP: horseradish peroxidase; AMEC: 3-amino-9-ethylcarbazole. The figure was created with BioRender.com.

required high-affinity antibodies through collaboration; 2) exploring label-free detection methods based on more advanced bare-silica platforms; and 3) further validation of the FO-BLI biosensor for MPXV using large-scale clinical samples.

5. Conclusion

The application of the cSP-based FO-BLI platform demonstrated the effectiveness of cSP in rapidly and sensitively detecting MPXV

in clinical settings, with a remarkably low LOD achieved in both serum and saliva samples. The adaptability of this approach allows for facile customization by substituting virus-specific antibodies, thus enabling multi-virus detection without complex modification steps. The automation and multichannel capabilities of the FO-BLI system streamline the entire detection process, presenting a compelling case for high-throughput, automated, and rapid multi-virus detection. Additionally, the versatility of recombinant cSP extends beyond MPXV detection, offering potential applications in multiplexed biosensing and hardware development. Overall, cSP-based biosensors show significant promise for rapid and high-throughput viral detection.

CRediT authorship contribution statement

Xixi Song: Conceptualization, Formal analysis, Methodology, Validation, Writing – original draft, Writing – review & editing. **Ying Tao:** Resources, Validation, Writing – original draft, Writing – review & editing. **Sumin Bian:** Resources, Conceptualization, Funding acquisition, Methodology, Supervision, Validation, Writing – review & editing. **Mohamad Sawan:** Conceptualization, Funding acquisition, Supervision, Validation, Writing – review & editing.

Declaration of competing interest

The authors declare that there are no conflicts of interest.

Acknowledgments

This research was supported by Westlake University, China (Startup funds), the Research Center for Industries of the Future of Westlake University, China (Grant No.: WU2022C040), and the National Natural Science Foundation of China (Grant No.: 82104122).

Appendix A. Supplementary data

Supplementary data to this article can be found online at https://doi.org/10.1016/j.jpha.2024.100995.

References

[1] E. Morales-Narváez, C. Dincer, The impact of biosensing in a pandemic outbreak: COVID-19, Biosens. Bioelectron. 163 (2020), 112274.
[2] World Health Organization, 2022–23 Mpox (Monkeypox) outbreak, Global trends. https://worldhealthorg.shinyapps.io/mpx_global/. (Accessed 19 December 2023).
[3] F.-M. Lum, A. Torres-Ruesta, M.Z. Tay, et al., Monkeypox: Disease epidemiology, host immunity and clinical interventions, Nat. Rev. Immunol. 22 (2022) 597–613.
[4] I. Gul, C. Liu, X. Yuan, et al., Current and perspective sensing methods for monkeypox virus, Bioengineering (Basel) 9 (2022), 571.
[5] P. Halvaei, S. Zandi, M. Zandi, Biosensor as a novel alternative approach for early diagnosis of monkeypox virus, Int. J. Surg. 109 (2023) 50–52.
[6] G. Rabbani, M.E. Khan, A.U. Khan, et al., Label-free and ultrasensitive electrochemical transferrin detection biosensor based on a glassy carbon electrode and gold nanoparticles, Int. J. Biol. Macromol. 256 (2024), 128312.
[7] G. Rabbani, M.E. Khan, E. Ahmad, et al., Serum CRP biomarker detection by using carbon nanotube field-effect transistor (CNT-FET) immunosensor, Bioelectrochemistry 153 (2023), 108493.
[8] Y. Zheng, S. Bian, J. Sun, et al., Label-free LSPR-vertical microcavity biosensor for on-site SARS-CoV-2 detection, Biosensors 12 (2022), 151.
[9] M. Mathelié-Guinlet, T. Cohen-Bouhacina, I. Gammoudi, et al., Silica nanoparticles-assisted electrochemical biosensor for the rapid, sensitive and specific detection of *Escherichia coli*, Sens. Actuat. B Chem. 292 (2019) 314–320.
[10] X. Zhang, Y. Zhang, X. Zhang, et al., Interface design and dielectric response behavior of SiO_2/PB composites with low dielectric constant and ultra-low dielectric loss, Surf. Interfaces 22 (2021), 100807.
[11] L.S. Puumala, S.M. Grist, J.M. Morales, et al., Biofunctionalization of multiplexed silicon photonic biosensors, Biosensors (Basel) 13 (2023), 53.
[12] A. Sadiki, S.R. Vaidya, M. Abdollahi, et al., Site-specific conjugation of native antibody, Antib. Ther. 3 (2020) 271–284.
[13] D. Jeon, J.-C. Pyun, J. Jose, et al., A regenerative immunoaffinity layer based on the outer membrane of Z-domains autodisplaying *E. coli* for immunoassays and immunosensors, Sensors (Basel) 18 (2018), 4030.
[14] H.G. Lee, S. Kang, J.S. Lee, Binding characteristics of staphylococcal protein A and streptococcal protein G for fragment crystallizable portion of human immunoglobulin G, Comput. Struct. Biotechnol. J. 19 (2021) 3372–3383.
[15] X. Song, Z. Fredj, Y. Zheng, et al., Biosensors for waterborne virus detection: Challenges and strategies, J. Pharm. Anal. 13 (2023) 1252–1268.
[16] S. Kim, K.I. Joo, B.H. Jo, et al., Stability-controllable self-immobilization of carbonic anhydrase fused with a silica-binding tag onto diatom biosilica for enzymatic CO_2 capture and utilization, ACS Appl. Mater. Interfaces 12 (2020) 27055–27063.
[17] S. Bian, M. Shang, M. Sawan, Rapid biosensing SARS-CoV-2 antibodies in vaccinated healthy donors, Biosens. Bioelectron. 204 (2022), 114054.
[18] S. Bian, M. Shang, Y. Tao, et al., Dynamic profiling and prediction of antibody response to SARS-CoV-2 booster-inactivated vaccines by microsample-driven biosensor and machine learning, Vaccines 12 (2024), 352.
[19] Y. Tao, S. Bian, P. Wang, et al., Rapid optical biosensing of SARS-CoV-2 spike proteins in artificial samples, Sensors (Basel) 22 (2022), 3768.
[20] S. Bian, Y. Tao, Z. Zhu, et al., On-site biolayer interferometry-based biosensing of carbamazepine in whole blood of epileptic patients, Biosensors (Basel) 11 (2021), 516.
[21] B. Webb, A. Sali, Comparative protein structure modeling using MODELLER, Curr. Protoc. Bioinform 54 (2016) 5.6.1–5.6.37.
[22] A. Waterhouse, M. Bertoni, S. Bienert, et al., SWISS-MODEL: Homology modelling of protein structures and complexes, Nucleic Acids Res. 46 (2018) W296–W303.
[23] G. Studer, C. Rempfer, A.M. Waterhouse, et al., QMEANDisCo-distance constraints applied on model quality estimation, Bioinformatics 36 (2020), 2647.
[24] C. Liu, D.L. Steer, H. Song, et al., Superior binding of proteins on a silica surface: Physical insight into the synergetic contribution of polyhistidine and a silica-binding peptide, J. Phys. Chem. Lett. 13 (2022) 1609–1616.
[25] C. Zhang, L. Liu, H. Li, et al., An oriented antibody immobilization based electrochemical platform for detection of leptin in human with different body mass index, Sens. Actuat. B Chem. 353 (2022), 131074.
[26] J.B. Fishman, E.A. Berg, Protein A and protein G purification of antibodies, Cold Spring Harb Protoc. 2019. https://doi.org/10.1101/pdb.prot099143.
[27] Z. Zhang, H. Jiang, S. Jiang, et al., Rapid detection of the monkeypox virus genome and antigen proteins based on surface-enhanced Raman spectroscopy, ACS Appl. Mater. Interfaces 15 (2023) 34419–34426.
[28] L. Ye, X. Lei, X. Xu, et al., Gold-based paper for antigen detection of monkeypox virus, Analyst 148 (2023) 985–994.
[29] P. Cao, X. Lai, R. Zhang, et al., Fluorescent immunochromatographic assay (FICA) for monkeypox virus, Anal. Lett. 57 (2024) 2118–2131.
[30] C. Wang, Q. Yu, J. Li, et al., Colorimetric–fluorescent dual-signal enhancement immunochromatographic assay based on molybdenum disulfide-supported quantum dot nanosheets for the point-of-care testing of monkeypox virus, Chem. Eng. J. 472 (2023), 144889.
[31] Y. Zheng, X. Song, Z. Fredj, et al., Challenges and perspectives of multi-virus biosensing techniques: A review, Anal. Chim. Acta 1244 (2023), 340860.
[32] T. Ikeda, A. Kuroda, Why does the silica-binding protein "Si-tag" bind strongly to silica surfaces? Implications of conformational adaptation of the intrinsically disordered polypeptide to solid surfaces, Colloids Surf. B Biointerfaces 86 (2011) 359–363.